

# Structural, morphological, hydrophilic and optical study of as synthesized and annealed Cl doped CdZnS thin films

SURESH KUMAR<sup>1</sup>, AFTAB ALAM<sup>2</sup>, RAJEEV RANJAN<sup>3</sup>, S. R. KUMAR<sup>4</sup>, S. K. SHARMA<sup>5</sup>, K. P. TIWARY<sup>6,\*</sup>

<sup>1</sup>Department of Physics, Chaibasa Engineering College, Kelende, Jhinkpani, Jharkhand-833215, India

<sup>2</sup>Department of Engineering Physics, Al-Kabir Polytechnic, Mango Jamshedpur, Jharkhand-831012, India

<sup>3</sup>Department of Electronics and Communication Engineering, Birla Institute of Technology Mesra, Patna Campus, Patna-800014, India

<sup>4</sup>Department of Applied Science & Humanities, National Institute of Advanced Manufacturing Technology, Ranchi, Jharkhand-834003, India

<sup>5</sup>Department of Physics, Indian Institute of Technology (Indian School of Mines), Dhanbad, Jharkhand-826004, India

<sup>6</sup>Department of Physics, Birla Institute of Technology, Mesra, Patna Campus, Bihar-800014, India

Chemical bath deposition technique was used to create a thin film of chlorine doped CdZnS in a non-aqueous medium. Thiourea [SC(NH<sub>2</sub>)<sub>2</sub>], sodium chloride [NaCl], cadmium acetate [Cd(CH<sub>3</sub>CO<sub>2</sub>)<sub>2</sub>], and zinc sulphate [ZnSO<sub>4</sub>] were employed as precursors to develop Cl doped CdZnS thin films. The deposited film is annealed in air at 350°C. The films have been characterized by XRD, FESEM, EDS, WCA, Raman and FTIR. According to XRD study, while being deposited and annealed, Cl doped CdZnS films have hexagonal crystal structure with (002) preferred orientation. The evaluation of the numerous characteristics via XRD spectra includes grain size, micro strain and dislocation density. FESEM study shows that as deposited film surface exhibit fibre net arrangements, but after being annealed at 350°C, the surfaces are compact and fine-grained. WCA investigations verified that annealing makes the surface less hydrophilic. FTIR investigations verified the existence of various functional groups and chemical bonds.

(Received July 6, 2023; accepted February 12, 2024)

**Keywords:** XRD, FESEM, Non aqueous, Cl doped CdZnS, Thin films

## 1. Introduction

Solar energy can be taken as an important source of renewable energy which could be changed to electricity with the help of solar cells. Rapid increase in energy crisis develops a new dimension of research in the field of solar technology. These days, photovoltaic devices, phosphors, and photodetectors frequently use chalcogenide-based semiconducting materials [1,2]. Metal chalcogenide can be referred as a group of inorganic chemical compound which have one chalcogen anion and one more electropositive metal. Researchers have been interested in binary or ternary chalcogenide semiconductors because they can modify their characteristics to fulfill specific purposes for device development [3]. Chalcogenide semiconductors that are binary or ternary are of interest to science because their characteristics can be modified to satisfy certain needs when fabricating devices. Mixed compound semiconductors of group II-VI, III-V, IV-VI like CdSe, CdS, Cd<sub>(1-x)</sub>Zn<sub>x</sub>S, Cd<sub>(1-x)</sub>Zn<sub>x</sub>Se, CdSe<sub>(1-x)</sub>Te<sub>x</sub>, In<sub>1-x</sub>Ga<sub>x</sub>Sd<sub>1-y</sub>As<sub>y</sub> have potential applications in the fabrication of photoconductive cells, photovoltaic cells, electronic and optoelectronic devices [4-10]. Since group II-VI compounds can produce ternary and quaternary alloys with a straight fundamental bandgap assignment over the full

alloy composition range and with high absorption coefficients, many researchers have focused on this group of compounds. The bandgap energy of CdZnS, a ternary II-VI combination, varies from 2.4 eV to 3.7 eV and is mostly based on the relative Cd:Zn ratios [11]. As a material for large bandgap windows, CdZnS thin films are commonly utilized in heterojunction solar cells, nanoelectronics, photonics, photoconductive devices, optoelectronic nanodevices, etc. Cl<sup>-</sup> ions can easily penetrate the crystal lattice of CdZnS because their ionic radius (1.81 Å) is slightly less than that of S<sup>2-</sup> (1.84 Å) ions. Influence of Chlorine content in the CdZnS film will increase the solar cell efficiency [12]. Thin films can be prepared using a variety of techniques, including spraying, chemical bath deposition, CVD, etc. Several researchers have reported Cl doped CdZnS thin films which was carried out in aqueous solution with the aid of chemical bath deposition process.

In this article, we present the CBD method for fabrication of Cl doped CdZnS thin films that were deposited on ITO glass substrates in non-aqueous solution. Non-aqueous baths provide more opportunities for deposition sources, a wider range of operating temperatures, and freedom from the ubiquitous hydrogen evolution reaction, which is sometimes a hassle in creating stress- and pinhole-free deposits [13]. The important

parameters studied here are structural (crystallite size and micro strain) surface morphological, elemental analysis, hydrophobicity nature, chemical bonding characteristics, etc.

## 2. Materials and methods

### 2.1. Cl doped CdZnS thin film preparation

The AR grade of Cadmium acetate  $[\text{Cd}(\text{CH}_3\text{CO}_2)_2]$  (0.40M) as a  $\text{Cd}^{2+}$  source, Zinc sulphate  $[\text{ZnSO}_4]$  (0.15M) as a  $\text{Zn}^{2+}$  source, and Sodium chloride  $[\text{NaCl}]$  (0.10M) as a Chlorine source were used to make the electrolyte, which was then dissolved in 75ml (1:2 ratio) of ethylene glycol and ethanol. All these precursors are in analytical reagent grade of purity (99% of Rankem) purchased from Oswal chemicals and Engineering, India. The electrolyte's temperature was held constant at  $130^\circ\text{C}$ . For one hour, the electrolyte was aged and continuous stirring was used to carry out the deposition. The substrate for the deposition of Cl doped CdZnS film was ITO glass. Before deposition the ITO glass plate was washed three times: first with boiling distilled water, then with hot soapy water and then with distilled water. A strong support was used to dip an ITO glass substrate into the electrolyte. Thiourea  $[\text{SC}(\text{NH}_2)_2]$  (0.27M) as an  $\text{S}^{2-}$  source was added to the electrolyte at time  $t=0$  while being stirred moderately at 220 rpm. After 20 minutes, the Cl-doped CdZnS film had a yellowish colour. Films are rinsed with distilled water for 25 seconds after deposition in order to get rid of organic contaminants and counter ions. Cl doped CdZnS films deposited on ITO glass substrate was physically stable and identify good adhesion. The prepared as-deposited Cl doped CdZnS films are annealed at  $350^\circ\text{C}$  in air.

### 2.2. Characterization of the films

The crystalline structure of the Cl doped CdZnS film as deposited was investigated using a X-ray diffractometer system (Make-Rigaku, Japan, Model-Smart Lab 9KW) ray source  $\text{CuK}_\alpha$ , radiation wavelengths of  $1.54\text{\AA}$  and scanning range of  $2\theta$  equals  $20^\circ$ -  $80^\circ$ . Using Debye- Scherrer's formula, the average grain size of Cl doped CdZnS nanocrystalline films were determined as they were being deposited and annealed. With the aid of a field emission scanning electron microscope (FESEM, Make-Carl Zeiss microscope Ltd., Germany, Model-Sigma 300) operating at 10,000KX magnifications, the surface morphology of the films was examined, and the elemental composition was calculated using an attached energy dispersive X-ray analyser (EDAX). The hydrophilic or hydrophobic character of the deposited films is determined using the water contact angle measurement technique, which is analysed utilising a water contact angle measuring apparatus (Make-Dataphysics, Germany, Model-OCAH 230). The Raman characteristics (Make-Renishaw inVia Raman Spectroscopy) were done using a Raman Spectroscopy with raman shift range of  $100\text{ cm}^{-1}$  to  $800\text{ cm}^{-1}$ . The FTIR examination was done using a Shimadzu spectrometer with a wave number range of  $500\text{ cm}^{-1}$  to  $4000\text{ cm}^{-1}$  (model number IR Prestige-21).

## 3. Result and discussions

### 3.1. XRD analysis

The polycrystalline character of the as-deposited and annealed Cl doped CdZnS thin films over ITO glass is indicated by their XRD patterns, which are illustrated in Fig. 1.

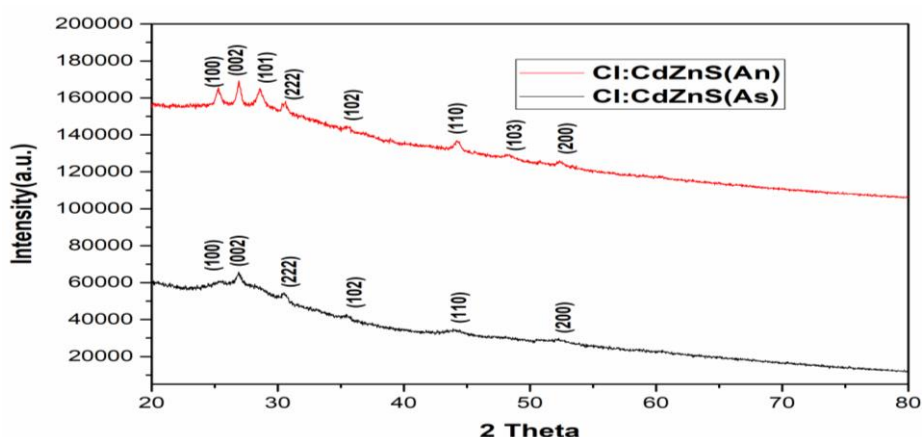


Fig. 1. XRD spectra of as deposited and annealed Cl-doped CdZnS thin films (color online)

The scan angle of the film is 20-80 degree at scan rate of  $3^\circ$  per minute. The spectra's peaks have all been detected and marked. As can be shown, both as deposited and annealed Cl doped CdZnS thin films with hexagonal structure have diffraction patterns located at  $2\theta=25.24^\circ$ ,  $26.91^\circ$  and  $35.58^\circ$  with indices of (100), (002), and (102)

planes, respectively, with a preference for orientation along the (002) plane. After annealing, it is seen that the planes (101) and (103) appear at  $28.56^\circ$  and  $48.27^\circ$ , respectively. Similar to this, the intensity of the annealed film's (100) and (002) diffraction peaks broadens and becomes more intense due, in part, to the abundance of defects [14]. The

reflections due to ITO glass substrate are at  $32^\circ$ ,  $44^\circ$ , and  $52^\circ$  correspond to the (222), (110), and (200) Miller planes for both films. The produced homogeneous, well-adhered Cl doped CdZnS thin films are achieved. The films microstructural characteristics, including crystallite size (D), micro strain ( $\epsilon$ ), and dislocation density ( $\delta$ ), were calculated using the following formulae as given in equations (1), (2) and (3).

$$D = \frac{0.94\lambda}{\beta \cos\theta} \quad (1)$$

$$\epsilon = \frac{\beta \cos\theta}{4} \quad (2)$$

$$\delta = \frac{1}{D^2} \quad (3)$$

where,  $\theta$  be the Bragg's angle,  $\beta$  is the full-width at half maximum of the (002) peak,  $\lambda$  is X-ray wavelength

The as-deposited and annealed Cl doped CdZnS thin films have calculated crystallite sizes of 22 nm and 38.50 nm, respectively. The improvement in crystallinity is obviously demonstrated by the rise in average grain size carried on by annealing. Table 1 below lists the typical grain size, microstrain ( $\epsilon$ ), and dislocation density of both as deposited and annealed Cl doped CdZnS films formed on ITO glass substrate.

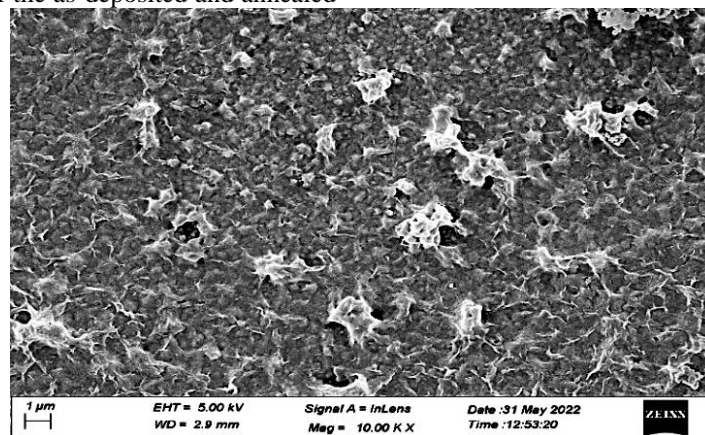
Table 1. Average grain size, Micro-strain and dislocation density of as deposited and annealed Cl doped CdZnS thin films

Sample	2 $\theta$	hkl plane	FWHM	Grain Size (D)	Micro strain ( $\epsilon$ )	Dislocation density ( $\delta$ )
Cl: CdZnS As deposited	26.91	002	0.3763	22 nm	$0.159 \times 10^{-3}$	$0.00206 \text{ (nm}^{-2}\text{)}$
Cl: CdZnS Annealed	26.94	002	0.2212	38.50 nm	$0.939 \times 10^{-3}$	$0.000674 \text{ (nm}^{-2}\text{)}$

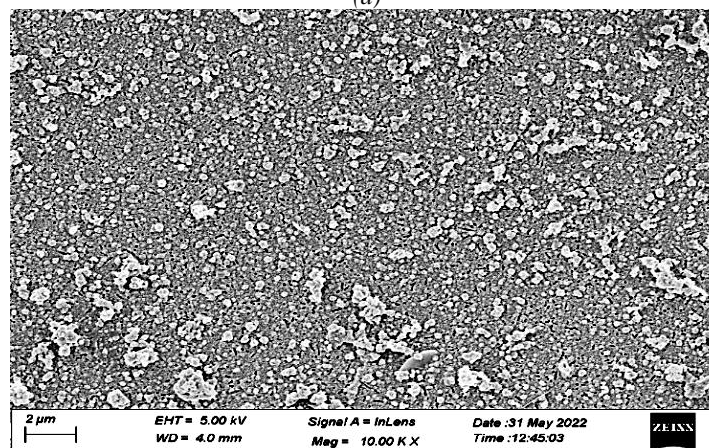
### 3.2. FESEM analysis

FESEM is a technique that has a lot of potential for studying the topography of materials and it provides crucial details about the way that particles grow and take on their shape. The morphologies of the as-deposited and annealed

Cl doped CdZnS thin films are clearly depicted in Fig. 2(a) and (b). For both films, a 10,000X magnification FESEM picture is taken. It is explained by the deposited film's smooth, dense, and uniform surface, which is lacking of pinholes or fractures.



(a)



(b)

Fig. 2. FESEM photograph of (a) as deposited and (b) annealed Cl-doped CdZnS thin films

One can see the uniform arrangement of grains covering the entire substrate from the micrograph. It is obvious that as deposited film, spheres with fibre net structures are seen. When film is annealed at 350<sup>o</sup>c, the surface of the film is modified, and spherically shaped grains are densely distributed in both single and cluster form throughout the studied area with a compact and fine-grained morphology. The principal reason for the grain cluster is the coalescence of smaller grains [15].

### 3.3. Elemental analysis

The EDS spectra of Cl-doped CdZnS thin films as they were deposited and annealed are shown in Fig. 3(a) and (b), which show the clearly defined peaks for Cd, Zn, S, and Cl.

In as-deposited and annealed Cl doped CdZnS thin films, the quantitative atomic and weight percentages of the compositional constituents such as Cd, Zn, S, and Cl are shown in Table 2. It is evident that the atomic elemental ratio of Zn is lower than the Cd ratio, which is in good agreement to Zhou et al. [16]. Table 2 demonstrates that both Cl doped CdZnS films are sulfur-rich and that the ratio of the atomic percentages of S and Cd for as deposited and annealed films were 1.2 and 1.3. Due to surface contamination a sulfur-rich oxygen peak is also possible. Additionally, it can be inferred from Table 2 that the incorporation of Cl into CdZnS films is supported by the growing tendency of the annealed film's atomic percentage of Cl, which can be seen by EDS measurements.

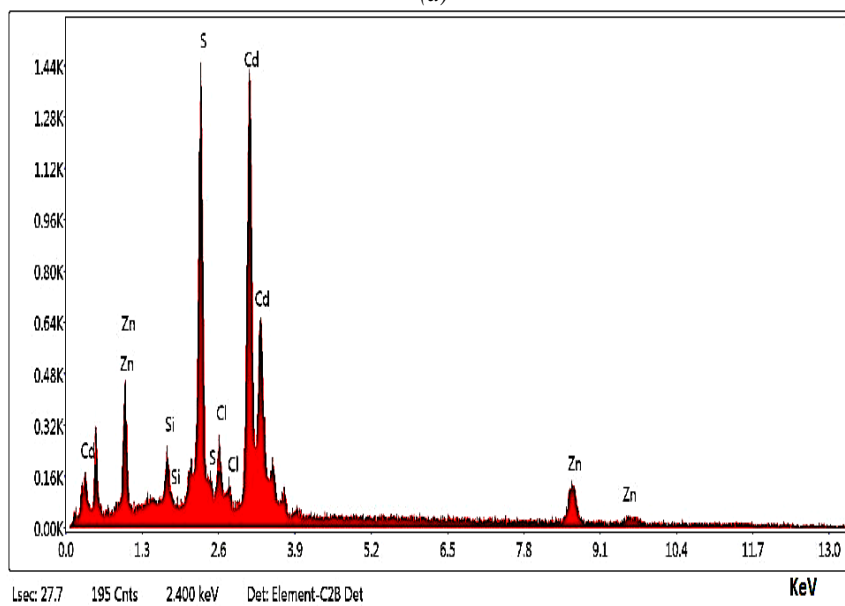
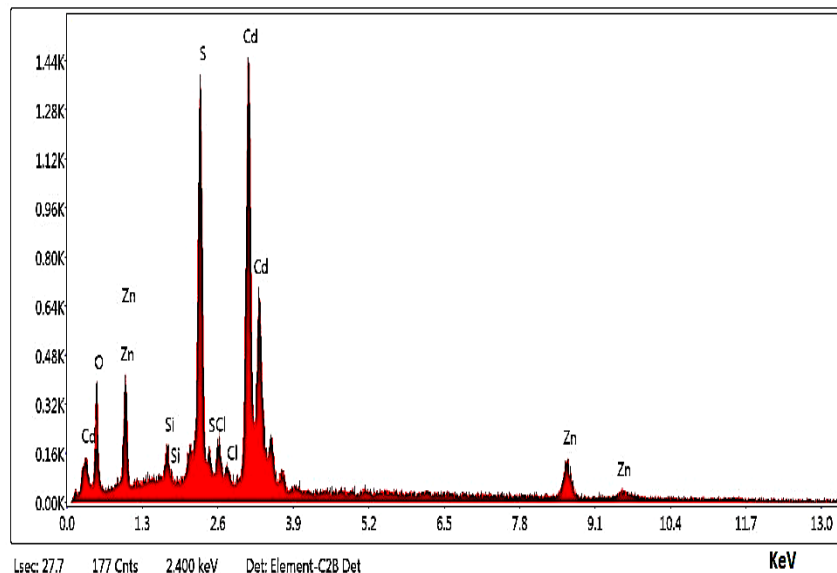


Fig. 3. EDS spectra of (a) as deposited and (b) annealed Cl-doped CdZnS thin films (color online)

Table 2. Elemental composition values of as deposited and annealed Cl doped CdZnS thin films

Sample	Elemental Composition (At% and Wt%)											
	Cd		Zn		S		Cl		O		Si	
	At.%	Wt.%	At.%	Wt.%	At.%	Wt.%	At.%	Wt.%	At.%	Wt.%	At.%	Wt.%
Cl:CdZnS (As-deposited)	20.7	50.45	10.27	14.55	26.48	18.41	3.11	2.39	37.45	12.99	1.99	1.21
Cl:CdZnS (Annealed)	31.43	56.56	15.4	16.12	41.71	21.41	6.37	3.61	-	-	5.09	2.29

### 3.4. Wettability studies

Water contact angle measurement ( $\theta$ ) is used in wettability studies to describe the surface's wetting nature. The important characteristics of a solid surface that determine the relationship between water droplets and its surface are hydrophobicity and hydrophilicity. When wettability is high, contact angle will be low ( $\theta < 90^\circ$ ), indicating a

hydrophilic surface [17], while when wettability is low, contact angle will be high ( $\theta > 90^\circ$ ), indicating a hydrophobic surface [18]. Fig. 4 (a) suggests that the contact angle for as-deposited Cl doped CdZnS film is  $68.17^\circ$ , indicating that the film should be hydrophilic in nature. However, Fig. 4 (b) shows that the contact angle should be  $77.35^\circ$  for annealed film. According to this study, it may be concluded that annealing makes the surface less hydrophilic.

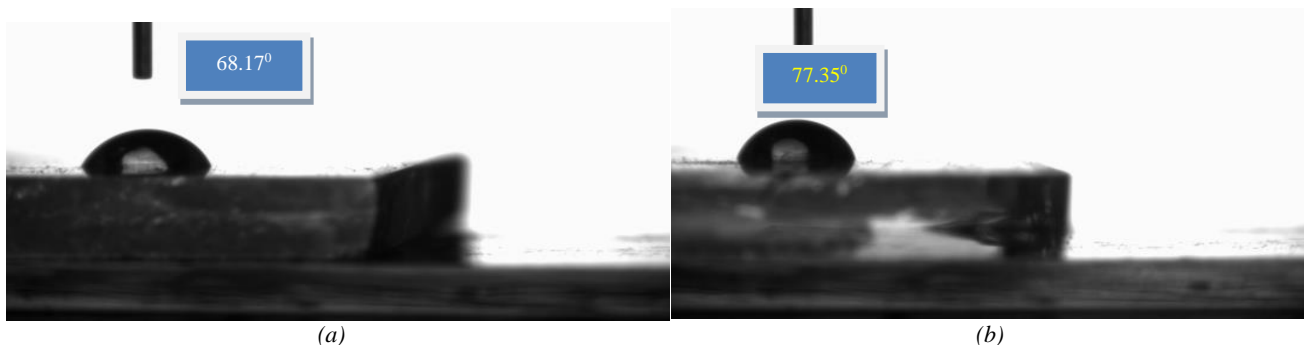


Fig. 4. WCA image of (a) as deposited and (b) annealed Cl-doped CdZnS thin films (color online)

### 3.5. Raman studies

One of the crucial instruments for studying multi exciton materials as a probe of the exciton-photon coupling via the Frohlich interaction is Raman spectroscopy [19]. It is well known that Raman scattering spectra provide helpful details on the location of the spectral peak and the spectral width attributable to the film's crystallinity [20]. Fig. 5

shows the Raman spectra of as deposited and annealed Cl doped CdZnS thin films deposited on ITO glass substrate at room temperature in the visible range  $100$  and  $800\text{ cm}^{-1}$  which revealed two modes: 1LO and 2LO. These modes of both the films were observed around  $300\text{ cm}^{-1}$  and  $603\text{ cm}^{-1}$  in the spectra. Longitudinal optical (LO) mode is linked to the first peak, whereas its first overtone is linked to the second peak [21].

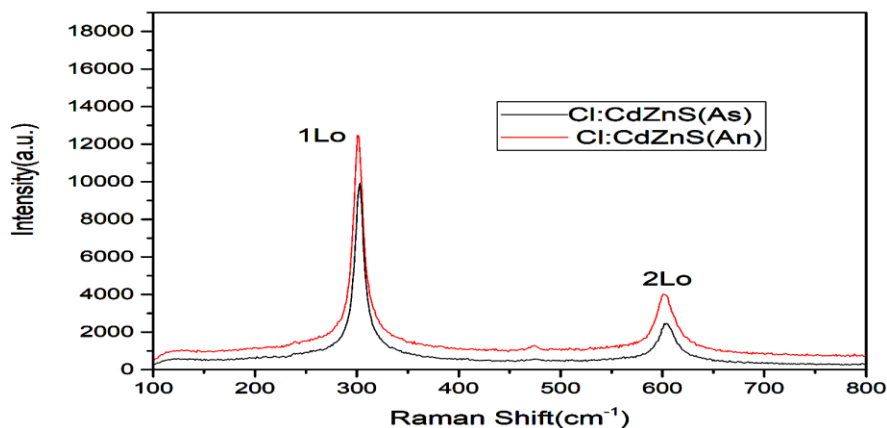


Fig. 5. Raman spectra of as deposited and annealed Cl-doped CdZnS thin films (color online)

Surface optical phonon (SOP) mode effect is responsible for both films' first order longitudinal optical (1LO) mode [22]. A highly crystalline material is present, as indicated by the presence of the 1LO and 2LO phonon modes. The Raman spectra was found to include overtones

with lesser intensities than the fundamental wavelength [23], which is in good accord with other studies on CdS nanoparticles from Rajalakshmi et al. [24], Zhang et al. [25], and Oladeji et al. [26].

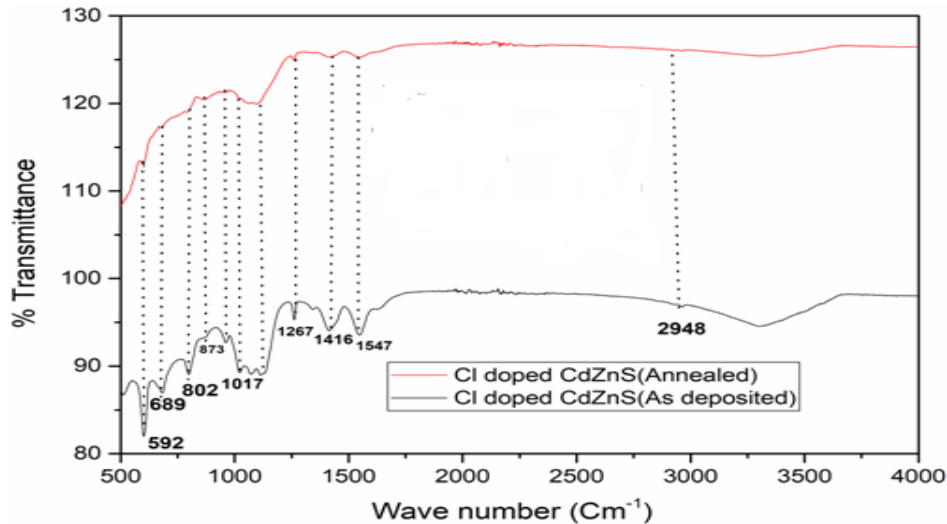


Fig. 6. FTIR spectra of as deposited and annealed Cl-doped CdZnS thin films (color online)

### 3.6. FTIR studies

Fig. 6 shows the results of an FTIR analysis of Cl doped CdZnS films that were grown over an ITO glass substrate and then annealed. All peaks in the spectra of the aforementioned films were detected after analysis using a spectrometer in the wavenumber range of  $500\text{cm}^{-1}$  to  $4000\text{cm}^{-1}$ . The peak that formed at  $2948\text{cm}^{-1}$  on the graph can be attributable to C-H stretching vibration, which suggests the existence of species on the surface of nanocrystals [27]. Peaks at  $1547\text{cm}^{-1}$  and  $1416\text{cm}^{-1}$  demonstrate the vibrational mode of OH bending and asymmetric stretching, respectively, which is assigned to the vibrational mode of OH bending. A peak at  $1017\text{cm}^{-1}$  and  $1267\text{cm}^{-1}$  [28, 29] indicates the C-O stretching vibration of absorbed ethylene glycol. At  $873\text{cm}^{-1}$ , the weak peaks caused by C-H bending vibrations are seen. The Cd-S stretching vibration is indicated by the peak at  $689\text{cm}^{-1}$ .

## 4. Conclusions

Thin films of CdZnS doped with chlorine are promising candidates for usage in a variety of applications, such as solar cells and other optoelectronic devices. Using a chemical bath deposition approach in a non-aqueous solution, chlorine doped CdZnS thin films have been successfully formed on an ITO glass substrate at bath temperature  $130^{\circ}\text{C}$  after being annealed at  $350^{\circ}\text{C}$ . Both films have strong adhesion and are homogeneous. The deposition of Cl doped CdZnS thin films is polycrystalline, according to X-ray diffraction study. The computed

structural properties of both films include grain size, microstrain, and dislocation density. The computed and reported average grain sizes for both films are  $22\text{nm}$  and  $38.50\text{nm}$ , respectively. EDS analysis provided proof that elemental components were present. Raman spectra show that 1LO and 2LO modes were seen in the spectra at about  $300\text{cm}^{-1}$  and  $603\text{cm}^{-1}$ , respectively. The O-H stretching and the H-O-H bending are visible in FTIR spectra. The most desirable characteristics for optoelectronic applications, especially as window layers in solar cells, have been identified in the developed Cl doped CdZnS films.

### Acknowledgements

The authors appreciate having access to the laboratories at Birla Institute of Technology, Mesra, Ranchi and Chaibasa Engineering College's Material Research Laboratory and Central Instrument Facility, respectively.

### References

- [1] S. A. Al Kuhaimi, Z. Tulbah, Journal of the Electrochemical Society **147**(1), 214 (2000).
- [2] D. Lilhare, S. Pillai, J. Sci. Engg. Educ. **1**, 17 (2016).
- [3] M. Husain, B. P. Singh, S. Kumar, T. P. Sharma, P. J. Sebastian, Solar energy materials and solar cells **76**(3), 399 (2003).
- [4] K. P. Tiwary, S. K. Choubey, K. Sharma, Chalcogenide Letters **10**(9), 319 (2013).
- [5] Bo Che, Dongfang Yang, A. P. Charpentier,

- Suwas Nikumb, *Solar Energy Materials and Solar Cells* **9**, 1025 (2008).
- [6] R. Ranjan, C. M. S. Negi, K. P. Tiwary, *Chalcogenide Letters* **20**(4), 251(2023).
- [7] S. Kumar, K. P. Tiwary, *Emerging Trends in Nanotechnology*, Springer Nature, Singapore, 185 (2021).
- [8] R. Ranjan, C. M. S. Negi, S. K. Choubey, K. P. Tiwary, *Chalcogenide Letters* **20**(10), 709 (2023).
- [9] K. P. Tiwary, F. Ali, R. K. Mishra, S. K. Choubey, K. Sharma, *Journal of Ovonic Research* **16**(4), 235 (2020).
- [10] K. P. Tiwary, F. Ali, S. K. Choubey, R. K. Mishra, K. Sharma, *Optik* **227**, 166045 (2021).
- [11] S. K. Kulkarni, U. Winkler, N. Deshmukh, *Applied surface science*, **17**, 438 (2010).
- [12] G. Selvan, M. P. Abubacker, A. R. Balu, *Optik* **127**(12), 4943 (2016).
- [13] S. R. Kumar, R. B. Gore, S. K. Kulkarni, R. K. Pandey, *Thin Solid Films* **208**, 161 (1992).
- [14] S. Chandramohan, T. Strache, S. N. Sarangi, R. Sathyamoorthy, T. Soma, *Materials Science and Engineering B* **171**, 16 (2010).
- [15] A. Mukherjee, P. Ghosh, A. A. Aboud, P. Mitra, *Materials Chemistry and Physics* **184**, 101 (2016).
- [16] J. Zhou, X. Wu, G. Teeter, B. To, Y. Yan, R. G. Dhere, T. A. Gessert, *Phys. Stat. Sol. B* **241**(3), 775 (2004).
- [17] Sanjay A. Gawali, C. H. Bhosale, *Materials Chemistry and Physics* **129**, 751 (2011).
- [18] S. Rajpal, V. Bandyopadhyay, *Journal of Nano-and Electronic Physics* **5**(3), 03021 (2013).
- [19] B. Tell, B. T. C. Damen, S. P. S. Porto, *Phys. Rev.* **144**, 771 (1966).
- [20] Tuley Ozer, Sabita Akasy, Salih Kose, *Sci. Semicond. Proc.* **13**, 325 (2010).
- [21] G. L. Song, S. Guo, X. X. Wang, Z. S. Li, B. S. Zou, H. M. Fan, R. B. Liu, *New J. Phys.* **17**, 063024 (2015).
- [22] W. C. Chou, A. Pertou, J. Warnock, B. T. Jonker, *Phys. Rev. B Condens. Matter* **46**, 4316 (1992).
- [23] N. B. Colthup, L. H. Daly, S. E. Wiberley, *Introduction to Infrared and Raman Spectroscopy*, New York: Academic Press, 1964.
- [24] M. Rajalakshmi, T. Sakuntala, A. K. Arora, *J. Phys. Condens. Matter* **9**, 9745 (1997).
- [25] H. Zhang, D. Yang, X. Ma, Y. Ji, S. Li, D. Que, *Mater. Chem. Phys.* **93**, 65(2005).
- [26] I. O. Oladeji, L. Chow, J. R. Liu, W. K. Chu, A. N. P. Bustamante, C. Fredricksen, A. F. Schulte, *Thin Solid Films* **359**, 154 (2000).
- [27] Suresh Kumar, S. K. Sharma, Shashikant Rajpal, S. R. Kumar, D. Roy, *Digest Journal of Nanomaterials and Biostructures* **12**(2), 339 (2017).
- [28] A. Alam, S. Kumar, D. K. Singh, *Materials Today: Proceedings* **62**, 6102 (2022).
- [29] S. R. Kumar, Suresh Kumar, S. K. Sharma, D. Roy, *Materials Today: Proceedings* **2**, 4563 (2015).

---

\*Corresponding author: kptiwary@bitmesra.ac.in